A Unified Picture of the Local Dynamics of Poly(dimethylsiloxane) across the Melting Point

Valeria Arrighi,* Simona Gagliardi, and Chuhong Zhang

Chemistry, School of Engineering and Physical Sciences, Heriot-Watt University, EH14 4AS Edinburgh, UK

Fabio Ganazzoli

Dipartimento di Chimica, Materiali e Ing. Chimica "Giulio Natta", Sez. Chimica Politecnico di Milano via L. Mancinelli 7, 20131 Milano, Italy

Julia S. Higgins

Department of Chemical Engineering and Chemical Technology, Imperial College, South Kensington Campus, London, SW7 2AZ, UK

Raffaella Ocone

Chemical Engineering, School of Engineering and Physical Sciences, Heriot-Watt University, EH14 4AS Edinburgh, UK

Mark T. F. Telling

ISIS, Rutherford Appleton Laboratory, Chilton, Didcot, OX11 OQX, UK

Received June 20, 2003; Revised Manuscript Received September 24, 2003

ABSTRACT: The local dynamics of poly(dimethylsiloxane) (PDMS) has been investigated by quasi-elastic neutron scattering (QENS). Methyl group reorientations dominate the QENS spectra up to 215 K (i.e., below the melting temperature, $T_m \approx 235$ K). The dynamics of the CH_3 groups is interpreted in terms of a model function consisting of elastic and quasi-elastic components, the latter given by a Gaussian distribution of Lorentzian lines. Above T_m, the QENS spectra are analyzed considering two processes: (a) the methyl group rotation and (b) the segmental motion. The activation energy for the latter is 14.6 kJ/mol, in excellent agreement with rheological data. Moreover, in agreement with the latter, the intermediate scattering function, $I(Q,t)$, computed via the inverse Fourier transform, follows time−temperature superposition according to the rheological shift factor. The contribution of the segmental motion to the scattering function $I(Q,t)$ was fitted with a stretched exponential function (or its Fourier transform in the frequency domain). The fitted stretching exponent β for segmental motion is 0.61 in both frequency and time domain, much higher than 0.5 (Rouse model), but in agreement with theoretical results realistically accounting for the chain stiffness. QENS studies of segmental motion in PDMS had indicated that the experimental data followed the Rouse model up to a very large Q, well beyond the validity range of the model. We suggest that the rotational motion of the methyl groups is responsible for this observation.

1. Introduction

Chain connectivity is a characteristic feature of polymer chains that is responsible for their unique physical and mechanical properties such as the viscoelastic behavior of melts, solutions, and rubbers. In contrast to small molecules, the motion of long, covalently bonded monomer units takes place over a wide time and length interval, from the monomeric to the overall molecular scale. Two temperature regimes can be distinguished. Bulk polymers in the solid state below the glass transition temperature, T_g, display a series of relaxation processes that are detected by dielectric spectroscopy, NMR, or dynamic mechanical thermal analysis.[1] These relaxations determine to a large extent the mechanical behavior of polymers. From a molecular viewpoint, high-frequency torsional and vibrational motions of side groups as well as small-amplitude backbone oscillations may contribute to the observed sub-T_g relaxations. These processes are localized, and unlike motions occurring above T_g, they do not lead to diffusion along the main-chain backbone.

On a local scale, molecular motion of polymer melts considerably deviates from the simple Brownian diffusion of small molecules. Chain connectivity leads to the definition of an important length scale: the critical chain length, R_e, above which entanglements with neighboring molecules determine flow properties. Long, entangled chains are well represented by the reptation model developed by de Gennes.[2] For shorter chains or at observation scales shorter than R_e, chain dynamics is well described by the Rouse model, which considers a chain as a sequence of beads connected by entropy springs of length b (b is of the order of several monomer units).[3] These two models offer a simple theoretical description of chain dynamics which leads to universal equations valid up to length scales where the details of the chemical structure of the monomers remain unimportant.

One of the limitations in the present understanding of chain dynamics is due to the inability to describe polymer motion, at length scale where the universal

* Corresponding author: e-mail v.arrighi@hw.ac.uk, Tel +44-(0)131 451 3108, Fax +44(0)131 451 3180.

10.1021/ma034843x CCC: $25.00
Published on Web 10/23/2003

behavior breaks down. Often dynamic experiments make use of empirical functions, and although they are able to determine the characteristic time of the molecular motion, they give little information on the nature of the molecular process. However, by either considering theoretically developed model functions or, as shown recently, comparing experimental data and molecular dynamics simulations, it is possible to establish links between chemical structure, local dynamics, and physical properties in polymer melts.

In this work, we present a dynamic study of poly(dimethylsiloxane) (PDMS), a polymer that has been extensively investigated using various experimental techniques such as dielectric spectroscopy,[4] mechanical relaxation,[5] nuclear magnetic resonance,[6−8] light scattering,[9] and neutron scattering.[10−12] Our work focuses on investigations of local dynamics using quasi-elastic neutron scattering (QENS), a technique that provides information on molecular motion in the time range $10^{-13}-10^{-10}$ s and on a length scale up to ca. 15 Å.[11,13] This limits the technique to studies of fast local conformational transitions between isomeric states, librational motion, and rotations of side groups. We also report rheological measurements on the same samples, probing the slow dynamics of the chains and aiming to establish links between microscopic motion and macroscopic dynamic behavior.

Our measurements cover a wide temperature range so that we are able to follow the PDMS dynamics from the fast reorientational motion of the CH_3 groups occurring below the melting point, T_m, to the diffusive motion of the chain segments at $T > T_m$. Both methyl group rotation[14,15] and segmental dynamics[10−12] were previously investigated by neutron scattering.

Published results on the methyl group motion in PDMS at $T < T_m$ have neglected the existence of a distribution of rotational frequencies in the analysis.[14] However, as pointed out by some authors,[15] similarly to other polymers, a distribution of activation energies and/or rotational frequencies is required in order to account for the decrease of the elastic intensity in fixed window scan experiments and the non-Lorentzian shape of the quasi-elastic broadening. To characterize the fast CH_3 reorientational motion and evaluate its contribution at $T > T_m$ (T_m = 236 K), we performed QENS measurements in the range 100−215 K and analyzed the data in terms of a Gaussian distribution of rotational frequencies. We will show that up to T_m diffusive motion of the amorphous regions is too slow to be detected by QENS. Thus, up to T_m the methyl group motion provides the main contribution to the quasi-elastic broadening.

Segmental motion in PDMS melts has been extensively investigated using QENS. Early publications focused on the validity of the simple Rouse model in describing the intramolecular motion of unentangled chains.[16−18] The Rouse scattering law first calculated by de Gennes[19] leads to an intermediate scattering function $I(Q,t)$ for intramolecular dynamics within the range $R_e^{-1} < Q < b^{-1}$ of the form $\exp[-(t/\tau)^{0.5}]$, where τ is a Q-dependent characteristic time which is expected to vary as Q^{-4}. Both the predicted Q^{-4} dependence and the $t^{0.5}$ power law of the intermediate scattering function were confirmed experimentally for PDMS chains by neutron spin-echo[20] and quasi-elastic neutron scattering[17] measurements.

However, at large Q values, the Rouse model which was originally developed for a bead-and-spring chain should become unrealistic. At $Q > b^{-1}$ the exponential decay of the intermediate scattering function should give rise to a Lorentzian shape of the QENS broadening. Concomitantly, the Q dependence of the characteristic time should display a change from Q^{-4} to Q^{-2} as expected for the diffusion of single beads free from connectivity constraints. These deviations should be observable within the time and distance range probed by neutron scattering and particularly through QENS measurements. Indeed, deviations from the predicted Q^{-4} dependence were observed for other polymers,[17] including for instance polyisobutylene and poly(propylene oxide), but it is surprising to find that the PDMS data reported by Allen et al.[17] show Rouse behavior up to $Q = 1$ Å^{-1}, that is, up to distances of the order of the chemical bond length. One report exists where a crossover region from the large-scale Rouse behavior with a Q^{-4} dependence to the local motion with a Q^{-2} dependence at $Q = 0.15$ Å^{-1} was observed.[18] This result from measurements of single-chain dynamics is in disagreement with the work carried out by Allen et al.[17] and a recent report[21] where the NSE data of bulk PDMS were shown to follow Rouse predictions up to $Q = 0.40$ Å^{-1}.

A previous QENS study carried out by us on PDMS in the Q range up to 1.9 Å^{-1} has shown that the intermediate scattering function can be represented by a stretched exponential, $\exp[-(t/\tau_s)^{\beta}]$.[22] The β parameter was found to be Q and temperature independent and equal to 0.45, a result that is inexplicable in terms of the $t^{0.5}$ dependence predicted for the Rouse model due to the very small distance scale probed. In fact, $\beta = 0.5$ is the theoretical lower limit of the stretching exponent predicted for the very flexible chain of the Rouse model, any conformational stiffness leading to a larger β value.[23]

For larger momentum transfers, the theoretical validity of the Rouse model, or of any coarse-grained model, breaks down. The limitations of the Rouse model have been extensively discussed in the literature,[24] and theoretical developments have been made to extend the range of applicability of the model toward the small distance range, close to the monomeric scale.[25−29] Among the different approaches adopted, we recall coarse-grained models which account for the chain stiffness in terms of local correlations among the springs and more realistic models that consider the specific stereochemistry.[25−29] In a recent publication,[23] the shortcomings of the Rouse model were reviewed by some of us and the theoretical results from coarse-grained and realistic chains revisited by fitting the calculated $I(Q,t)$ curves with the empirical stretched exponential or Kohlraush−Williams−Watts (KWW) function. For PDMS, fitting of the theoretical $I(Q,t)$ curve determined for realistic, nonentangled PDMS chains within the rotational isomeric states (RIS) scheme leads to β values that are significantly larger than 0.5 (Rouse model) at short distances. That work provides a starting point to the analysis that is presented here, and therefore the main conclusions will be briefly given in the theoretical section.

A communication of the work to be presented has recently appeared in the literature.[30] In this paper, we report a detailed analysis of the PDMS data across the melting temperature and in a Q region where the Rouse model is no longer valid. We show that the results of the analysis are model dependent. By accounting for the fast CH_3 group, we have isolated the contribution of the

segmental relaxation, and we show that the observed scattering is consistent with theoretical predictions which consider the conformational details of the polymer chain in terms of the RIS scheme. In addition, the temperature dependence of the intermediate scattering function is fully reproduced by the rheological shift factors.

In the next section, we discuss some of the theoretical aspects related to the characterization of the polymer dynamics by QENS, followed by a brief review of the Rouse model and a discussion of the factors that should lead to deviations from this model when approaching small length scales. A more detailed description can be found in ref 23. Experimental details are reported in section 3. The results of the data analysis are presented in three different sections. First we describe the window scan data analysis, second we deal with the dynamics of the methyl groups as monitored by QENS measurements below the melting point, and finally we combine all information and propose a model that describes molecular motion above T_m. Comparison between the temperature dependence of the segmental dynamics from QENS and from viscosity data is given in section 4.2.3. In section 5 we present a discussion of the results and comparison with literature data while brief conclusions to the work are given in section 6.

2. Theory

2.1. Molecular Motion by QENS.[11,13] Polymeric materials generally contain a large number of hydrogen atoms. Because of the large incoherent cross section of hydrogen ($\sigma_{inc}(H) = 80.26$ barn) with respect to that of other nuclei, the total scattering cross section can be approximated to the incoherent scattering cross section, σ_{inc}. For PDMS, this equals to 481.6 barn, which is much larger than the coherent cross section ($\sigma_{coh}(H) = 28.4$ barn). By assuming that the coherent scattering can be neglected, the following equations will solely refer to incoherent scattering.

In a neutron scattering experiment aimed to study molecular motion, the scattered intensity is measured as a function of both energy and momentum transfer, Q ($Q = (4\pi/\lambda)\sin(\theta/2)$, where λ is the neutron wavelength and θ is the scattering angle). One then defines the double differential scattering cross section, $\partial^2\sigma/(\partial E\,\partial\Omega)$, as the probability that a neutron is scattered with energy change ΔE into the solid angle $\Delta\Omega$. This quantity is related to the incoherent scattering law, $S_{inc}(Q,\omega)$, through the relationship

$$\left(\frac{\partial^2\sigma}{\partial\Omega\,\partial E}\right)_{inc} = \frac{Nk}{k_0}\Delta b^2 S_{inc}(Q,\omega) \qquad (1)$$

where N is the number of atoms while k and k_0 represent the magnitude of the scattered and incident wave vectors ($k = 2\pi/\lambda$), respectively. The term Δb^2 depends on fluctuations of the scattering length b due to the presence of different isotopes, and it is related to the incoherent cross section ($\sigma_{inc} = 4\pi\Delta b^2$).

The incoherent scattering law, $S_{inc}(Q,\omega)$, conveys dynamic information on the system under study. This is shown by the following equations where $S_{inc}(Q,\omega)$ is written as the time-Fourier transform of the intermediate scattering function $I_{inc}(Q,t)$ describing correlations between the positions of the same scattering nuclei at time zero and t:

$$S_{inc}(Q,\omega) = \frac{1}{2\pi}\int I_{inc}(Q,t)\exp(-i\omega t)\,dt \qquad (2)$$

$$I_{inc}(Q,t) = \frac{1}{N}\sum\langle\exp(iQR_i(t))\exp(-iQR_i(0))\rangle \qquad (3)$$

where the brackets indicate a thermal average and $R_i(t)$ and $R_i(0)$ represent the position of the ith nucleus ($i = 1, 2, \ldots, N$) at time t and $t = 0$, respectively.

Depending on the temperature and experimental energy range, the measured dynamic incoherent structure factor $S_{inc}(Q,\omega)$ may need to be expressed as a convolution of different processes:

$$S_{inc}(Q,\omega) = S_{inc}^{trans}(Q,\omega) \otimes S_{inc}^{rot}(Q,\omega) \otimes S_{inc}^{vib}(Q,\omega) \qquad (4)$$

for example vibrations, rotations, and translations of the scattering centers. It follows from this equation that the intermediate scattering function is given by the product of the different dynamic contributions

$$I_{inc}(Q,t) = I_{inc}^{trans}(Q,t)\, I_{inc}^{rot}(Q,t)\, I_{inc}^{vib}(Q,t) \qquad (5)$$

Equations 4 and 5 are valid if the assumption of dynamically decoupled molecular motion holds.

A convenient way to separate rotational motion and segmental diffusive processes is to carry out measurements at sufficiently low temperature where the backbone chain motion is frozen in. This implies temperatures below the polymer glass transition for an amorphous system or below T_m for a semicrystalline material such as the PDMS sample investigated here.

In general, there is no translational contribution below the glass transition temperature and therefore, for polymers containing side groups, the scattering law coincides with the rotational scattering law of the side groups:

$$S_{inc}^{rot}(Q,\omega) = A_0(Q)\,\delta(\omega) + S_{inc}^{qel}(Q,\omega) \qquad (6)$$

where $A_0(Q)$ is the elastic incoherent structure factor (EISF), which represents the space-Fourier transform of the final distribution of the scatters, averaged over all possible initial positions. For a 3-fold rotation, $A_0(Q)$ is given by

$$A_0(Q) = \frac{1}{3}(1 + 2j_0(\sqrt{3}Qr)) \qquad (7)$$

where $j_0(x)$ is a zero-order spherical Bessel function and r is the distance between the moving protons and the rotation axis.

If vibrational and rotational motion are dynamically decoupled, then it can be shown that the only vibrational contribution to the quasi-elastic scattering is through the Debye−Waller factor (DWF).[12,13] (In practice, the validity of this assumption depends on the time scale of the spectrometer used.) Thus, eq 6 becomes

$$S_{inc}(Q,\omega) = DWF[A_0(Q)\,\delta(\omega) + S_{inc}^{qel}(Q,\omega)] \qquad (8)$$

For an amorphous polymer, the quasi-elastic incoherent component is described by a log-Gaussian distribution of Lorentzian lines $L_i(\omega)$.[31−33]

$$S_{inc}^{qel}(Q,\omega) = [1 - A_0(Q)]\sum g_i L_i(\omega) \qquad (9)$$

where $L_i(\omega) = (1/\pi)[\Gamma_i/(\Gamma_i^2 + \omega^2)]$. This arises from

differences between intermolecular interactions and packing in amorphous systems, which lead to a distribution of barrier heights for the rotational motion, as a result of which different groups rotate with different frequencies. The weight of each Lorentzian line g_i is determined from

$$g(\ln \Gamma_i) = \frac{1}{(2\pi\sigma_\Gamma{}^2)^{0.5}} \exp\left[\frac{-(\ln \Gamma_i - \ln \Gamma_0)^2}{2\sigma_\Gamma{}^2}\right] \quad (10)$$

In our analysis of CH_3 group rotations in poly(methyl methacrylate) (PMMA) and poly(vinyl methyl ether) (PVME)[33] we have used a different procedure to the one described above. After deconvolution of the experimental QENS data to derive the intermediate scattering function, the latter was analyzed using a stretched exponential or Kohlrausch−Williams−Watts (KWW) function.[34,35] In this paper, consistent with NMR and QENS analyses of side-group rotations in polymers, we account for the non-Lorentzian shape of the quasi-elastic broadening via a log-Gaussian distribution of correlation times. A similar procedure has been employed in NMR and QENS studies of methyl[31,36−38] and phenylene group motions.[39] Although both methods satisfactorily describe the dynamic behavior of glassy polymers,[39,40] there are advantages in using a log-Gaussian distribution of correlation times or rotational frequencies to analyze $I(Q,t)$ or $S(Q,\omega)$, respectively, namely that the distribution of activation energies is easily derived from the data.[31]

Above the glass transition temperature or the melting point, the elastic line due to a fixed center of mass broadens. It is now customary to describe local melt dynamics in terms of the Fourier transform of the KWW (eq 11) or equivalent expressions such as the Havriliak−Negami function.[24,41,42] Rigorously, for a polymer containing side groups, the dynamic incoherent structure factor at $T > T_m$ should be expressed by the convolution of two functions relative to translational and rotational motion. This procedure has been used to analyze the influence of the CH_3 dynamics on the incoherent dynamic structure factor computed from MD simulations carried out on polyisoprene above T_g.[43] However, most of the QENS experimental data at $T > T_g$ (or T_m) use a single, often empirical, model function to describe the observed dynamics and to extract information on the characteristic time of the molecular motion. When measurements are performed at very high temperature, where the contribution from side-group reorientations is merely a flat background, this is a good approximation, but as it will be discussed later, this is not the case here.

PDMS has a very low glass transition temperature; segmental motion is fast and can be investigated at room temperature on QENS spectrometers of different energy resolutions.[16,17,22] It is the purpose of this paper to discuss the influence of the relatively fast CH_3 motion on the dynamics probed by QENS at $T > T_m$.

2.2. Intramolecular Dynamics−Diffusive Segmental Motion. The internal dynamics of a polymer molecule in the range $R_e^{-1} < Q < b^{-1}$ can be successfully described by the simple Rouse model.[3] The scattering law derived by de Gennes[19] leads, in the long-time limit, to the following relationship for the intermediate scattering function:

$$I(Q,t) = \exp\left[-Q^2 \frac{b^2}{3}\left(\frac{W}{\pi} t\right)^{0.5}\right] \quad (11)$$

where b is the polymer step length and W^{-1} is a correlation time.[11] This is related to the segment friction coefficient ζ_0:

$$W = \frac{3k_B T}{\zeta_0 b^2} = 3D_{\text{eff}} \frac{N}{b^2} \quad (12)$$

with k_B being the Boltzmann constant and D_{eff} the Rouse diffusion coefficient which is equal to $D_{\text{eff}} = k_B T/N\zeta_0$. The $t^{0.5}$ dependence in eq 12 arises from the constraint to the motion exerted by the neighbors along the same chain to each segment.

From the above equations one expects the characteristic time to follow a Q^{-4} dependence, with the corresponding full width at half-height, fwhh, of the quasi-elastic component varying as Q^4. At high Q ($Q > b^{-1}$) a Brownian type of motion of simple beads with a Lorentzian scattering law and a Q^2 dependence is predicted. As pointed out by several authors,[17,23] such simple behavior is not experimentally observed due both to the local chain stiffness and to the observation length scales being smaller than b.

Accordingly, extensions beyond the Rouse model can be grouped in two sets: (i) coarse-grained models accounting for the chain stiffness in terms of idealized freely rotating (discrete) or wormlike (continuous) chain models;[23,26] (ii) realistic models accounting for the local stereochemistry of the specific polymer.[23,25,27−29,44,45] The latter approach, based on a realistic model of the local chain conformation, relies on the rotational isomeric states (RIS) scheme proposed long ago by Flory[46] to describe the equilibrium properties of unperturbed polymer chains. Such a description was later applied to dynamical studies by Allegra et al.[25,27−29] Within this model, the appropriate torsion angles and the chemical bond lengths and angles are correctly accounted for. In particular, considering the correlation between pairs of adjacent rotational states, their joint probabilities are obtained from their relative energies. In this way, the Rouse picture of noncorrelated Hookean springs transmitting elastic forces between first neighbors only is replaced by a more sophisticated representation of forces among all the backbone atoms with ideal springs having a force constant that decreases with topological separation. The traditional description of the chain dynamics in terms of normal modes of motions is still valid, but we get a mode-dependent force constant that depends on the generalized characteristic ratio C_p, p being the mode index. For the collective modes with $p \ll N$, C_p becomes asymptotically equal to the usual characteristic ratio C_∞. In the Rouse model, $C_p \equiv 1$, but for freely rotating and realistic chains it has a more complicated expression. The relevant equations for calculating both the coherent and the incoherent dynamic structure factor were reported in a number of papers[23,25,27−29] and are not duplicated here for brevity.

The final result for the scattering laws can only be given through lengthy expressions that can be easily evaluated numerically. The theoretical curves can be fitted by KWW stretched exponential functions, which satisfactorily reproduce the calculated line shapes down to $I(Q,t)/I(Q,0) \approx 0.05$.[23] In freely rotating chains, we

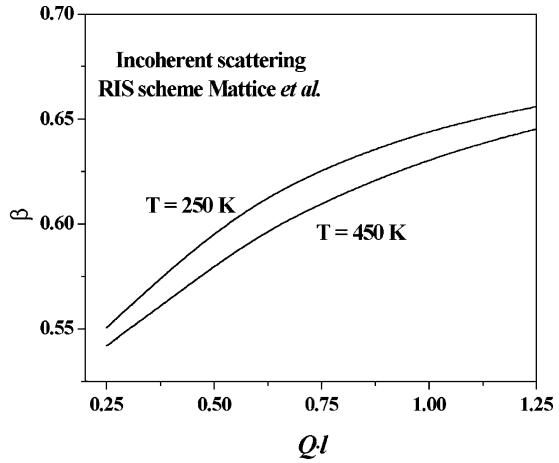

Figure 1. Theoretical β exponent for PDMS determined by fitting the calculated $I(Q,t)$ curves for incoherent scattering in the high-Q region (RIS scheme of Bahar et al.[48]) using a KWW function. The β parameter is plotted vs Ql, where l is the monomer length, equal to 2.9 Å for PDMS.[23] Calculations were carried out at two different temperatures, as indicated, and are independent of chain length within the reported Q range.

found that the stretching exponent β increases with chain stiffness above the 0.5 value of the original Rouse model. The parameter β is weakly Q dependent, though leveling off at large Q before reaching the limiting value of 1 due to the single-bead diffusion.

The theoretical results for PDMS in the high-Q region reported in Figure 1 were obtained adopting the RIS model proposed by Mattice et al.[47,48] This model, based on accurate molecular dynamics simulations, differs from the earlier one proposed by Flory, Crescenzi, and Mark[49] in that it better accounts for the unusually large flexibility of PDMS. However, one should note that our dynamical approach still treats the monomeric units as rigid entities, which introduces some inaccuracies at the largest Q values.

3. Experimental Section

3.1. Materials. The molecular weight of the poly(dimethylsiloxane) (PDMS) sample from Hopkin and Williams was 92 000 g/mol (viscosity grade: 30 000 cP). Differential scanning calorimetry (DSC) measurements performed on a Polymer Laboratories DSC at a heating rate of 10 °C/min give the following transitions: glass transition (T_g) at 148 K, cold crystallization at 182 K, and melting (T_m) at 230 and 236 K.

3.2. Neutron Experiments. Neutron scattering measurements were performed on the backscattering spectrometer IRIS at ISIS (Rutherford Appleton Laboratory, UK), on the high-resolution IN10 instrument at ILL (Grenoble, France), and on the QENS spectrometer (IPNS, Argonne National Laboratory).

3.2.1. QENS Measurements. For IRIS measurements, we used the PG(002) analyzer, giving an energy resolution of 15 μeV (measured as fwhh). Two experiments were performed on IRIS, covering the temperature range 4 to 300 K. Different setups were adopted so that the energy range covered in the measurements was (a) −0.2 to 1.2 meV (offset) and (b) −0.4 to 0.4 meV. For all measurements, the Q range varied from 0.25 to 1.9 Å^{-1}.

Quasi-elastic neutron scattering experiments were also carried out on the QENS spectrometer. The energy resolution of this instrument was ca. 70 μeV. The instrumental setup used during the experiment allowed data to be collected at three different Q values: 0.9, 1.88, and 2.4 Å^{-1}.

Data analysis was carried out according to RAL and IPNS routines in order to obtain the dynamic structure factor $S(Q,\omega)$ as a function of energy transfer. Data were corrected for transmission and absorption using software available at the neutron facilities, e.g., GUIDE at ISIS.[50] Fourier transformation of the frequency data was performed using a RAL routine, FURY,[51] as described in our previous publication.[33]

3.2.2. Fixed-Window Scans.[32] Incoherent elastic neutron scattering measurements were carried out on the spectrometer IN10[52] using the fixed-window technique. This instrument has a 1 μeV resolution ($t_{max} = 2 \times 10^{-9}$ s) at the full width of half-peak height and an accessible Q range from 0.5 to 1.96 Å^{-1}.

The neutron intensity scattered within a small energy window ($\Delta E \approx 1$ μeV) centered at $\omega = 0$ was monitored as a function of temperature (2−400 K) and scattering vector Q. The elastic scattering was normalized to the extrapolated value at 0 K in order to obtain $S(Q,\omega\approx0)(T)/S(Q,\omega\approx0)(T\approx0)$.

In the absence of rotational and translational motion, the molecular vibrations give rise to a decrease of the elastic intensity with increasing temperature, which is expressed by the Debye−Waller factor. If rotational motion takes place, the observed elastic scattering can be determined from[14,53]

$$S(Q,\omega\approx0) = A_0(Q) + \frac{2}{\pi}[1 - A_0(Q)]\ \mathrm{arctg}\left(\frac{\Gamma_r}{\Gamma}\right) \qquad (13)$$

where Γ_r is the width of the resolution function and Γ is the width of the Lorentzian line characterizing the quasi-elastic broadening. The latter parameter is temperature dependent and usually described by the Arrhenius law:

$$\Gamma = \Gamma_\infty \exp\left(-\frac{E_a}{RT}\right) \qquad (14)$$

It was noted earlier that a distribution of activation energies has to be invoked to account for the decay of the elastic intensity and the non-Lorentzian shape of the quasi-elastic broadening. Similarly to our previous publication, we have used a Gaussian distribution of activation energies:[32,53]

$$g_i = \frac{1}{(2\pi\sigma_E^{\,2})^{0.5}} \exp\left[-\frac{(E_i - E_0)^2}{2\sigma_E^{\,2}}\right] \qquad (15)$$

where g_i gives the weight of Gaussian distribution of activation energy and σ_E is the width of the distribution of activation energies while E_0 gives the center of the distribution. The normalized incoherent elastic intensity was then fitted to[53]

$$S(Q,\omega\approx0) = \left\{A_0(Q) + [1 - A_0(Q)]\sum_i g_i \frac{2}{\pi}\ \mathrm{arctg}\left[\frac{\Gamma_r}{\Gamma_\infty \exp(-E_i/RT)}\right]\right\}\mathrm{DWF} \qquad (16)$$

If the Debye−Waller factor is known, the decrease of elastic intensity leads to the determination of the activation energy and distribution and the EISF, i.e., $A_0(Q)$ in eq 16.

3.3. Rheological Measurements. The bulk viscosities of 11 PDMS samples with different molecular weight (in the range 236−92 000 g/mol) were measured using a CSL 100 controlled stress rheometer. All tests were conducted using a cone and plate. The cone diameter was 4.0 cm for high molecular weight samples and 6.0 cm for low molecular weight samples, and the gap at the tip of the cone was 0.054 mm for the former while 0.056 mm for the latter. In both cases angles were equal to 1.59°.

4. Results

4.1. Analysis of Fixed-Window Scan Data. In Figure 2, we report the decrease of the normalized elastic scattered intensity $[S(Q,\omega\approx0)(T)/S(Q,\omega\approx0)(T=0)]$ as a function of temperature as measured on IN10 at different Q values. As noted earlier,[32] the temperature

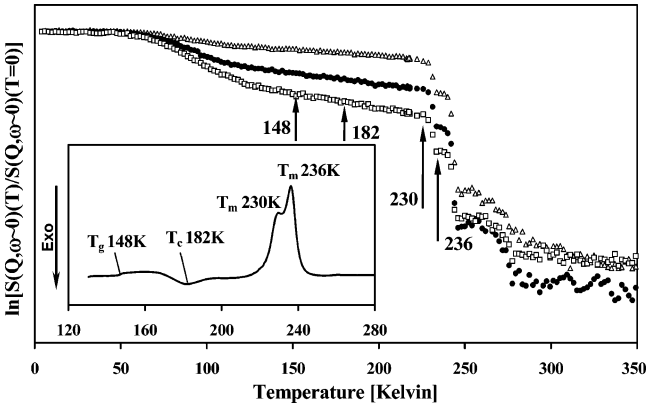

Figure 2. Temperature dependence of the normalized elastic incoherent structure factor, $\ln[S(Q,\omega\approx0)(T)/S(Q,\omega\approx0)(T=0)]$ of PDMS at (△) 0.86, (●) 1.43, and (□) 1.82 Å^{-1}. The glass transition (T_g), cold crystallization (T_c), and melting temperatures (T_m) are indicated in the graph. These correspond to thermal transitions observed calorimetrically (in the inset: DSC trace).

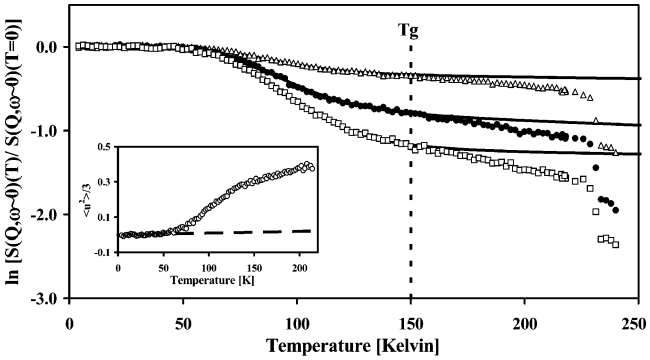

Figure 3. Temperature dependence of the normalized elastic incoherent structure factor, $\ln[S(Q,\omega\approx0)(T)/S(Q,\omega\approx0)(T=0)]$, at (△) 0.86, (●) 1.43, and (□) 1.82 Å^{-1}. The dashed line marks the glass transition whereas the continuous lines represent fits to the experimental data using eq 16. In the inset: effective mean-squared displacement as a function of temperature. The dashed line gives the temperature dependence $\langle u^2\rangle$ used in the fits.

dependence of the elastic window scans mimics the thermal behavior of PDMS observed by differential scanning calorimetry (see the inset in the same figure).

Below 55 K, a linear decrease of $\ln[S(Q,\omega\approx0)(T)/S(Q,\omega\approx0)(T=0)]$ with increasing temperature is observed, which is described by the Debye−Waller factor:

$$\frac{S(Q,\omega\approx0)(T)}{S(Q,\omega\approx0)(T=0)} \propto e^{-\langle u^2\rangle Q^2/3} \qquad (17)$$

where $\langle u^2\rangle$ is the mean-square amplitude of vibrations which increases linearly with increasing temperature, i.e., $\langle u^2\rangle \propto T$. Therefore, by plotting $\ln[S(Q,\omega\approx0)(T)/S(Q,\omega\approx0)(T=0)]$ vs temperature, any nonlinearity observed is due to molecular motions other than vibrations. In the temperature range 60−150 K, the decrease of the elastic intensity beyond the normal Debye−Waller factor is attributed to the reorientational motion of the methyl groups.

For fully amorphous polymers, a large decrease of the elastic intensity is observed at temperatures above the glass transition (for PDMS, $T_g = 148$ K). However, since PDMS is a semicrystalline material, the elastic intensity decreases little until the temperature exceeds the melting point ($T_m \sim 236$ K) (Figure 2). Above 230 K, the decrease of $\ln[S(Q,\omega\approx0)(T)/S(Q,\omega\approx0)(T=0)]$ perfectly reproduces the two thermal transitions (melting endotherms) observed by DSC. At $T > T_m$, the elastic intensity decreases sharply, indicating fast molecular motion as expected from a sample which is, in this temperature range, at least 100 deg above its glass transition.

The Q dependence of the elastic intensity vs temperature profiles is simply accounted for by the Q-dependent elastic incoherent structure factor, $A_0(Q)$, and although this was considered as a fitting parameter, the results are in good agreement with calculations for a 3-fold rotation.

The $\ln[S(Q,\omega\approx0)(T)/S(Q,\omega\approx0)(T=0)]$ vs temperature profiles were fitted to eq 16, using as fitting parameters the most probable activation energy E_0, the width of the distribution of activation energy σ_E, the elastic incoherent structure factor $A_0(Q)$, and attempt to escape frequency Γ_∞ as adjustable fitting parameters. From the fits shown in Figure 3 we obtained an average activation energy of 5.0 ± 0.1 kJ mol^{-1} with distribution 1.0 ± 0.2 kJ mol^{-1} and $\Gamma_\infty = 0.32 \pm 0.05$ meV, which are all Q independent parameters.

The mean-square amplitude of vibrations, $\langle u^2\rangle$, was evaluated from the Q dependence of the low-temperature window scan data, using eq 17. As shown in the inset of Figure 3, $\langle u^2\rangle$ varies linearly with temperature up to 55 K. We find that the temperature dependence of the mean-square displacement is equal to $d[\langle u^2(T)\rangle/3]/dT = (2.5 \pm 0.5) \times 10^{-4}$ Å^2/K, a value which is consistent with those reported for other polymers.[32]

A point worth mentioning is that the deviations from experimental window scan data and fits are evident in Figure 3. These are likely to be due to motion of the rubbery amorphous regions in this semicrystalline polymer, a result that is supported by the IRIS data presented in the next section. Alternatively, one could argue that the fast process (of the order of picoseconds) normally observed in amorphous polymers could contribute to the observed deviations. In our experience, a pronounced fast process would be detected as a further decrease in the window scan data even at temperatures below T_g. This would have two main consequences on the data analysis: (1) data fitting using eq 16 would lead to lower $A_0(Q)$ values than expected for a simple 3-fold rotation, and (2) the effective mean-square displacement would show two distinct temperature dependencies before and after the steplike increase due to the CH_3 motion. As indicated earlier, the $A_0(Q)$ values determined from the fits are in good agreement with the expected values for a 3-fold rotation.

The results of the window scan IN10 data analysis are in good agreement with the QENS spectra measured on the IRIS spectrometer, which will be discussed in detail in the next session.

4.2. QENS Data Analysis. 4.2.1. Methyl Group Dynamics. Analysis of the window scan data has indicated that, in the temperature range T_g to T_m, there is limited motion taking place, except for the methyl group rotation. If the deviations between model and experimental data shown in Figure 3 at $T > T_g$ simply result from the slow motion of the amorphous regions, then similar deviations should take place at higher temperature on instruments with lower resolution (in this case IRIS) compared to IN10. Consequently, the incoherent dynamic structure factor, $S(Q,\omega)$, measured by QENS should be well represented by a single process i.e., the reorientation of the CH_3 groups.

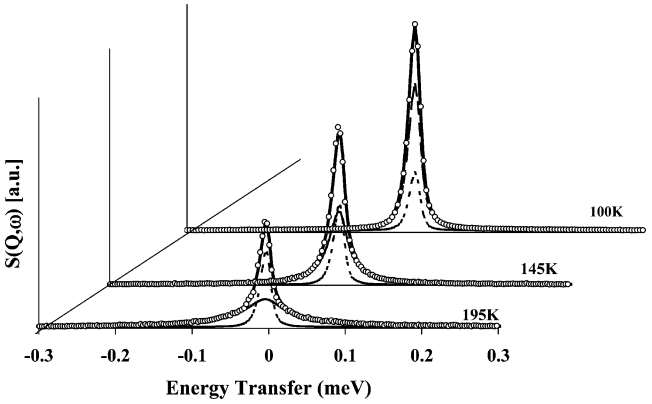

Figure 4. QENS spectra of PDMS at $Q = 1.84$ Å^{-1}: (○) experimental data and fits (solid line) using a model function consisting of an elastic component (dotted line) and a log-Gaussian distribution of Lorentzian lines (dashed line) convoluted with the instrumental resolution plus a flat background.

In agreement with the above conclusion, the dynamic incoherent structure factors measured on IRIS consist of two components: an elastic term (a delta function) and a quasi-elastic component, the latter defined as a log-Gaussian distribution of Lorentzian lines with width Γ_i and weight g_i (see eqs 8−10). This model function is convoluted with the instrumental resolution and, after addition of a flat background, fitted to the experimental data. The existence of a flat background in this energy range is a common feature of amorphous polymers which, as indicated by both experiments and MD simulations on various systems, is likely to be due to a fast picosecond process.

As shown in Figure 4 for $Q = 1.84$ Å^{-1}, this model describes the experimental scattering curves up to ca. 200 K, but deviations are observed at higher temperature ($T = 235$ K, not shown here). At any given temperature, the width of the distribution of rotational frequencies σ_Γ and the most probable width of the quasi-elastic component, Γ_0, are Q independent. The Q dependence is given by the elastic incoherent structure factor $A_0(Q)$ which, on the basis of the analysis of the window scan data, was taken to be equal to values calculated from eq 7 with $r = 1.032$ Å. As expected, Γ_0 follows an Arrhenius temperature dependence with activation energy 4.5 ± 0.5 kJ/mol. The paramater σ_Γ is temperature dependent, but the corresponding value for the distribution activation energies, $\sigma_E = 1.1 \pm 0.1$ kJ/mol, is constant in the range 100−200 K. The attempt to escape frequency is $\Gamma_\infty = 0.63$ meV. These results are in good agreement with the IN10 data analysis reported in the previous section.

For consistency with our previous work[33] and the time domain analysis that follows, the $S(Q,\omega)$ data collected at $T < T_m$ were Fourier transformed and analyzed in the time domain using a log-Gaussian distribution of correlation times. Here we note that there is very good agreement between the two analyses as indicated in Figure 5, thus confirming the good quality of the frequency data up to the largest energy exchanges. In the time domain, eqs 8 and 9 translate to a log-Gaussian distribution of exponential decays which tends, toward long times, to a Q dependent plateau, i.e., $A_0(Q)$. The most probable characteristic time of the motion, τ_0 (which corresponds to Γ_0), follows an Arrhenius temperature dependence with activation energy, E_a, equal to 4.6 kJ/mol. From the high-temperature limit $\tau_\infty = 1/\Gamma_\infty$

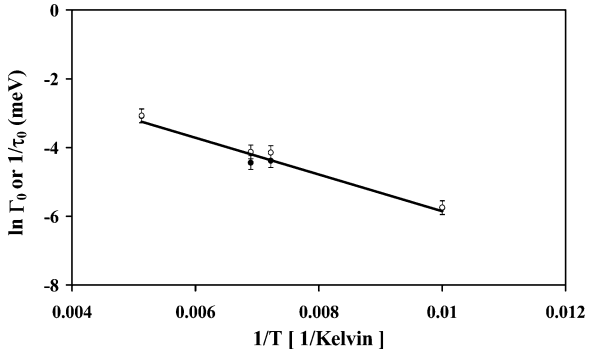

Figure 5. Temperature dependence of (●) Γ_0 from analysis of the $S(Q,\omega)$ data and (○) $1/\tau_0$ (meV) values extracted from analysis of the intermediate scattering functions. The line indicates interpolation through the experimental points using the Arrhenius equation.

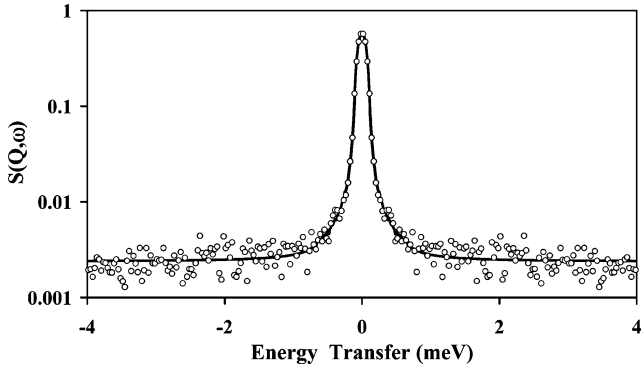

Figure 6. Quasi-elastic neutron scattering spectrum of PDMS at $Q = 1.88$ Å^{-1} and 140 K (QENS spectrometer): experimental data (○) and fit (solid line) using parameters extracted from measurements on IRIS.

we extract a value of Γ_∞ equal to 0.81 meV. Similarly to the energy domain analysis, from the distribution of characteristic times, which is temperature dependent, we obtain a temperature independent distribution of activation energies $\sigma_E = 1.3 \pm 0.3$ kJ/mol.

The parameters extracted from fits of the $S(Q,\omega)$ or $I(Q,t)$ data from the IRIS spectrometer are also representative of results obtained on spectrometers with lower resolution and wider energy range. This is shown in Figure 6 where the frequency data at $T = 140$ K are well reproduced using parameters determined from the IRIS data analysis. (An additional background is included that accounts for the existence of a fast process.) Additionally, as noted earlier for PMMA and PVME,[33] the intermediate scattering functions from IRIS and QENS show good overlap (Figure 7), thus confirming that the set of parameters reported here describe the CH_3 dynamics over a wide range of energy transfer.

4.2.2. Segmental Motion Dynamics. Up to 215 K the QENS experimental data are described by considering a single dynamic process, i.e., CH_3 reorientations. This is because, in the temperature range T_g to T_m, the segmental motion associated with the amorphous regions is too slow to be detected on the IRIS spectrometer. Thus, the only contribution to the quasi-elastic broadening arises from hopping of the CH_3 groups over the potential barrier.

Above T_m, the dynamics of PDMS is complicated by the absence of a fixed center of mass which gives rise to a further broadening of the elastic line. Usually, the QENS spectra of polymer melts are fitted using empirical model functions such as the KWW or by invoking

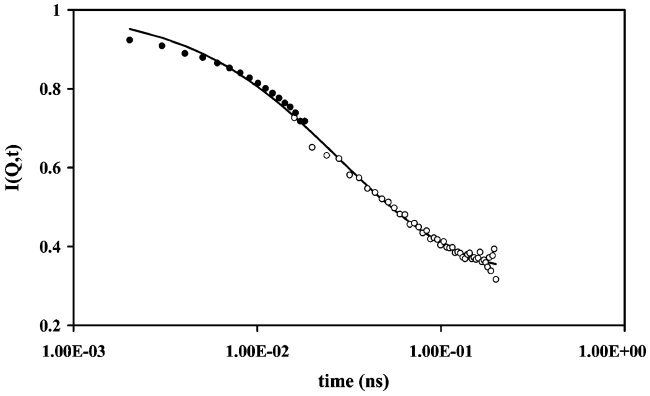

Figure 7. $I(Q,t)$ data of PDMS at 140 K and $Q = 1.88$ Å^{-1} from the QENS (●) and IRIS (○) spectrometers. The solid line is a fit to the combined data using a log-Gaussian distribution of exponentials.

the Rouse model. Both methods have limitations: the former is a purely empirical function while the latter describes the intramolecular motion of unentangled polymer chains, neglecting the details of the chemical structure which become important at short distances.

Despite these limitations, our first analysis of the IRIS data at $T > T_m$ was carried out using the Fourier transform of the KWW, $S_{KWW}(Q,\omega)$, to model the dynamic incoherent structure factor. In the time domain this model function is given by

$$I_{inc}(Q,t) = \exp\left[-\left(\frac{t}{\tau_s}\right)^{\beta}\right] \qquad (18)$$

where τ_s is a characteristic time that defines the segmental dynamics and β is the stretched exponent related to the distribution of relaxation times. An example of data fitting is given in Figure 8; analysis leads to a set of β values that suggest no apparent Q or temperature dependence (Figure 9), the average being equal to 0.45 but with a relatively large scatter of ±0.08. The characteristic time varies with Q^{-n} with n in the range 3.0−3.3, depending on temperature.

While this model adequately describes the shape of the $S(Q,\omega)$ curves, the results are at odds with theoretical calculations for PDMS chains which predict an increase of the stretched exponent β with increasing Q[23] compared to the minimum value of 0.5 for a Rouse chain. Furthermore, the results presented in the previous section have shown that few degrees below T_m methyl group rotations provide a nonnegligible contribution to the scattering. Therefore, in describing the dynamics of PDMS melts, it is necessary to consider a more complex model that accounts for the existence of two dynamic processes: (a) fast methyl group reorientation and (b) slow segmental motion.

The dynamic incoherent structure factor will therefore be given by convolution of two components:

$$S_{inc}(Q,\omega) = S_{inc}^{seg}(Q,\omega) \otimes S_{inc}^{rot}(Q,\omega) \qquad (19)$$

due to segmental motion and methyl group rotation. The former was expressed in terms of the Fourier transform of the KWW whereas the contribution of the CH_3 groups to $S(Q,\omega)$ was determined by extrapolation of the sub-T_m results to the desired temperature, considering Arrhenius behavior. The width of the distribution of Γ_i, σ_Γ, was calculated from the relationship $\sigma_\Gamma = \sigma_E/RT$ using the low-temperature data. This procedure which assumes no substantial change in the CH_3 motion below and above T_m appears to be supported by MD studies carried out on polyisoprene[43] which report similar distribution of activation energies for the CH_3 motion across T_g.

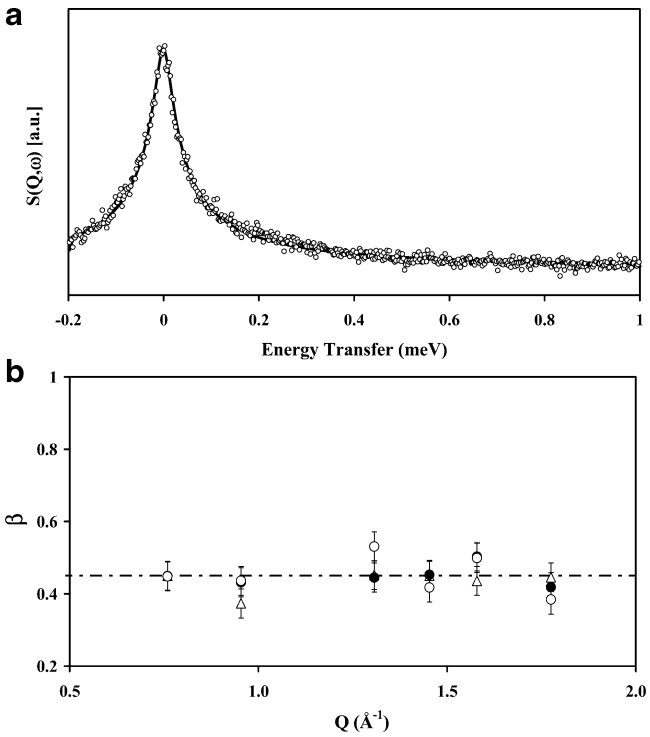

Figure 8. (a) QENS data of PDMS for $Q = 1.45$ Å^{-1} at 275 K: (○) experimental data, the line indicates a fit using as model function the Fourier transform of the KWW. (b) Q and temperature dependence of the β parameter: (△) 250 K, (●) 275 K, (○) 300 K.

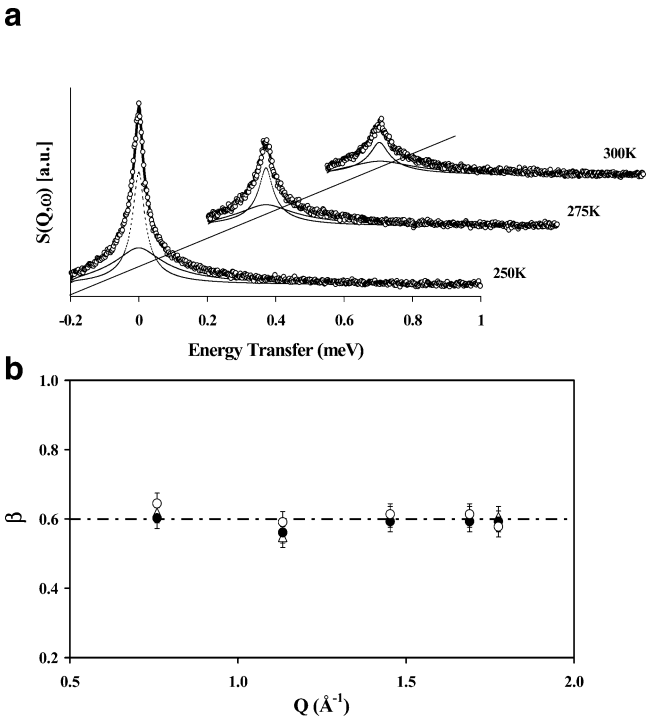

Figure 9. (a) QENS spectra of PDMS at $Q = 1.45$ Å^{-1} and selected temperatures (above T_m). Symbols represent experimental data, lines are fits using a model that consists of broad (dashed lines) and narrow components (dotted lines). (b) Q and temperature dependence of the β parameter: (△) 250 K, (●) 275 K, (○) 300 K.

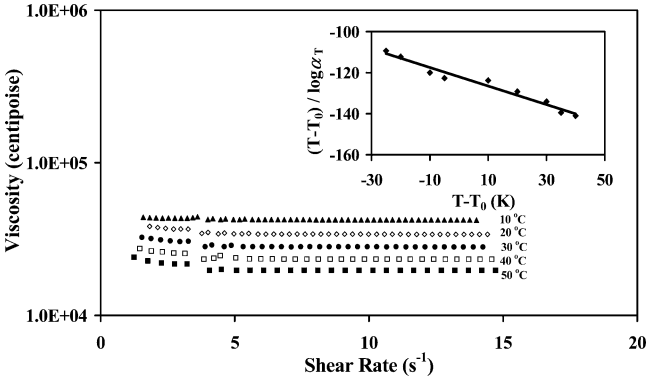

Figure 10. Temperature dependence of viscosity for a PDMS sample (92 000 g/mol) vs shear rate at different temperatures. In the inset: determination of the two empirical constants C_1 and C_2 of the WLF equation from a plot of $(T - T_0)/\log \alpha_T$ vs $(T - T_0)$.

Figure 9 gives examples of data fitting for $Q = 1.45$ Å^{-1} at three different temperatures, and similar results are obtained for other Q values. Although most of the parameters have been fixed (only τ_s and β are allowed to vary), the model reproduces well the experimental curves. As observed earlier for the single process fit, the inverse width of the quasi-elastic broadening relative to the slower process, τ_s, is Q dependent, i.e., $\tau_s = \tau_{eff}Q^{-n}$. In this case n is found to be ca. 2.3, a lower value compared to that obtained from the previous analysis. The τ_{eff} values follow an Arrhenius temperature dependence with an activation energy of 14.6 kJ/mol, in the temperature range 250−300 K.

Within experimental error, the β parameter of the KWW function characterizing the distribution of relaxation times is Q and T independent and equal to 0.61 with a scatter of about ±0.05 (Figure 9), significantly smaller than in the previous analysis. Thus, the effect of explicitly accounting for the faster reorientation of the methyl groups leads to a higher β value and to a lower Q dependence of τ_s.

4.2.3. Temperature Dependence of Segmental Motion. In this section we compare the temperature dependence of the incoherent dynamic structure factor at $T > T_m$ with data from rheological measurements.

Because of its high flexibility, the critical chain length of PDMS, defined as the onset of the entanglement formation leading to non-Newtonian behavior, is among the longest ones, ranging from about 660 to almost 1400 chain atoms.[54,55] The high molecular weight PDMS investigated here (92 000 g/mol) is above the critical chain length, and for this sample, two distinct ranges of Newtonian and non-Newtonian flow behavior separated by a critical shear rate around 100 s^{-1} are expected on the basis of measurements by Ghannam et al.[56] Thus, in performing the viscosity measurements, we controlled the shear rate below the critical value and then determined the temperature-dependent shift factor α_T (Figure 10). The latter was fitted to the Williams−Landel−Ferry (WLF) equation:[57]

$$\log \alpha_T = \log \frac{\eta(T)}{\eta(T_0)} = \log \frac{\tau(T)}{\tau(T_0)} = -\frac{C_1(T - T_0)}{C_2 + (T - T_0)} \quad (20)$$

By plotting $(T - T_0)/\log \alpha_T$ vs $(T - T_0)$ as shown in the inset of Figure 10, the two empirical constants C_1 and C_2 can be calculated from the slope and intercept. The calculated values for this sample are in good agreement with literature data ($C_1 = 1.90$ and $C_2 = 222$ K).[58]

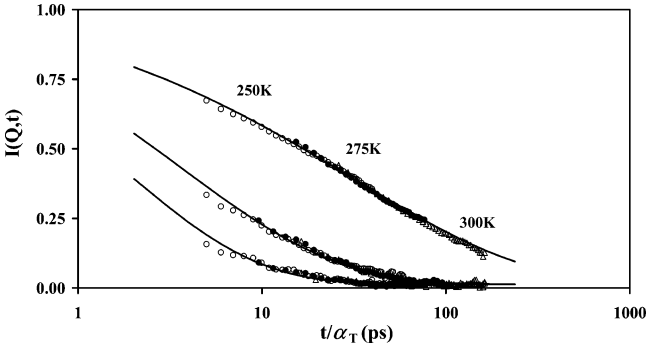

Figure 11. Time−temperature superposition of $I(Q,t)$ data at (○) 250, (●) 275, and (△) 300 K (reference temperature: 303 K). The Q values are 0.55, 1.13, and 1.58 Å^{-1} (from top to bottom). The lines correspond to fits to the experimental data (see text for details).

Although it is possible to extract WLF parameters from the data, one should note that the lowest temperature investigated is more than 100 deg above T_g, and so the temperature dependence of the viscosity is equally represented by an Arrhenius law. Our measurements show that the viscosity follows Arrhenius behavior; the flow activation energy increases with increasing molecular weight reaching a constant value of 14−15 kJ mol^{-1} for $M_w \gtrsim 3000$. This value is in very good agreement with the QENS data analysis presented in the previous section. Furthermore, the $I(Q,t)$ data computed from the $S(Q,\omega)$ spectra obey time−temperature superposition with shift factors that are in good agreement with rheological measurements. This is shown in Figure 11 for three selected Q values. The time-shifted $I(Q,t)$ data can be fitted using the same two-process model adopted to describe the $S(Q,\omega)$ curves, as indicated by the continuous lines reported in Figure 11. The fitting parameters are fully consistent with those reported for the frequency domain data analysis.

5. Discussion

The dynamics of PDMS has been widely investigated in the past, and both studies of methyl group rotation and segmental motion have been reported. In this section we compare our results with those reported in the literature.

Below the melting point, the dynamic process dominating the QENS spectra is due to hopping of the methyl groups across the potential barrier. The exact value of the potential barrier hindering CH_3 group rotations in PDMS has been the subject of discussion. For example, Henry and Safford[59] attributed the broad peak measured by inelastic neutron scattering at 160 cm^{-1} to the methyl group torsional motion. Because of its breadth, the reorientation of the CH_3 was considered to be almost free. A similar peak located at 165 cm^{-1} was observed by Allen et al.,[60] who calculated the height of the barrier hindering the rotational motion to be 6.9 kJ/mol, assuming a 3-fold potential. From measurements of the temperature dependence of the total cross section Amaral et al.[61] derived a value of 1.6 kJ/mol. Our QENS data gave an activation energy of 4.5 kJ/mol, and this result was consistently found independently from the chosen method of analysis and confirmed by using different spectrometers.

To our knowledge, no QENS data on methyl group dynamics have been reported in the literature except

for a preliminary study based on analysis of window scan data.[15,37] The results reported here differ from those in ref 37, mainly because in that work analysis of the window scan data was performed by assuming Γ_∞ to correspond to the frequency of the methyl group librational mode which for PDMS is located at 18.5 meV. While it is possible to fit our window scan data fixing Γ_∞ to 18.5 meV and extract a value of activation energy close to that reported, there would remain a large discrepancy between the analyses of dynamic incoherent structure factor and window scan (the former leads to lower Γ_∞ and E_a values). Furthermore, we note that at high temperature there is little difference between calculated Γ values using the two sets of fitting parameters.

We now discuss our results on the PDMS melt dynamics and review work reported in the literature. There have been extensive studies of the PDMS segmental dynamics by QENS as well as other techniques, e.g., NMR. Effective diffusion coefficients, D_{eff}, extracted from the neutron spectra assuming a Lorentzian line shape,[62−64] were reported for samples of different molecular weights as a function of temperature. After an initial decrease with chain length, D_{eff} reached a constant value of 2.1×10^{-9} m^2/s at room temperature for degrees of polymerization higher than 15. It was pointed out that these D_{eff} values, much larger than the corresponding ones from NMR spin-echo measurements, include at least one contribution above translational diffusion, which was associated with the reorientational motion of short segments of the polymer chain.[16,62−64] The temperature dependence of the effective diffusion coefficient was Arrhenius-like:

$$D_{eff} = D_0 \exp\left[-\frac{E_a}{RT}\right] \qquad (21)$$

with activation energy E_a equal to 7.5 kJ/mol,[64] but measured D_{eff} values were found to be resolution dependent.

It was later shown[16] that the resolution dependent D_{eff} values were a direct consequence of the non-Lorentzian shape of the quasi-elastic broadening and were therefore attributed to an incorrect choice of the scattering law $S(Q,\omega)$ used to fit the data. On the contrary, a Q^4-dependent broadening of the fwhh arising from a $t^{1/2}$ correlation function as in eq 11 was found to describe both low- and high-resolution experimental data.[16]

Similar investigations were carried out on other polymers: poly(tetrahydrofuran) (PTHF), poly(propylene oxide) (PPO), and poly(isobutylene) (PIB).[17] However, while PDMS was found to display a Q^4 dependence of the quasi-elastic broadening as expected o the basis of eq 11, all other polymers showed deviations from the predicted power law with values of the exponent $n < 4$. This behavior is not unexpected, and it arises from the short distance scale explored by QENS which is less than the statistical segment length.

These results seem to indicate that the Rouse model can be used to describe the segmental motion of PDMS in the QENS frequency range, but it was surprising to find that the Q^4 dependence extended well beyond the range of validity of the model itself. A Brownian motion of single beads with a Lorentzian scattering law would be expected at $Qb \geq 1$, where b is predicted to be of the order of 10 Å.

In this work, we have presented data from the IRIS spectrometer whose resolution (15 μeV) is intermediate between that of the spectrometers used in earlier studies. By first characterizing the low-temperature dynamics of the PDMS chains, we were able to show that, within the energy window of the IRIS spectrometer, the motion of the methyl groups cannot be neglected. Thus, we constructed a model function which, for temperatures above T_m, accounted for both methyl group rotations and segmental dynamics. In doing so, we assumed that the dynamics of the CH_3 groups could be described by the same model parameters below and above T_m.

The new model function used here led to a time dependence characterized by an exponent $\beta = 0.61$. This value, being larger than the lower limit 0.5 for the Rouse model, is consistent with theoretical predictions made by Ganazzoli et al.,[23] implying that on a very local scale some conformational rigidity can be detected. However, it must be noted that the β exponent remains quite small, as expected due to the very large flexibility of this polymer. Moreover, the value found here is in semiquantitative agreement with recent theoretical calculations, based on fitting the theoretically calculated $I(Q,t)$ curves for realistic, nonentangled PDMS chains within the RIS scheme to a KWW function (see Figure 1 and ref 23). For PDMS, the shape parameter β is predicted to be around 0.6, slowly increasing with increasing Q. We conclude that the local dynamics can be predicted by accounting both for the chain stiffness and for the underlying fast processes (the CH_3 rotation in the present case).

It is evident from our results that spectrometer resolution and energy range determine whether the methyl group rotation can/cannot be neglected. On a high-resolution spectrometer such as IN10 and at small Q values, one expects the contribution from methyl group rotations to be negligible. As observed experimentally, in these conditions, $\beta = 0.5$, and the quasi-elastic broadening follows a Q^4 power law.

6. Conclusions

We have reported a dynamic study of PDMS chains covering a wide temperature range, below and above the melting temperature. At $T < T_m$, the dynamics of PDMS is dominated by the rotational motion of the methyl groups. The quasi-elastic broadening has a non-Lorentzian line shape as observed previously for other polymers with CH_3 groups such as PVME and PMMA.

By extrapolating the low-temperature dynamics of PDMS to $T > T_m$, we demonstrated that the rotational motion of the methyl groups cannot be neglected, at least within the resolution and energy range of the IRIS spectrometer. The QENS data above 215 K have been described by a model which accounts for two processes: (a) a Q independent process due to the reorientation of the CH_3 groups and (b) a $Q^{2.3}$-dependent process associated with the local dynamics of the chains. For the latter, the scattering law was found to have a $t^{0.6}$ dependence, contrary to the $t^{0.5}$ predicted for the simple Rouse model. These results, i.e., $Q^{2.3}$ and $t^{0.6}$ dependencies, are supported by recent theoretical calculations realistically accounting for the local chain stiffness.[23]

Finally, the temperature dependence of the QENS data is in good agreement with expectations from rheological measurements. Similarly, the intermediate scattering functions follow the time−temperature su-

perposition, using the rheological shift factors. We note that this is not a trivial result. It lends further support to the conclusion that, although the chemical structure of the polymer becomes important at short distances, it is possible to achieve, at least for the flexible PDMS chains, a unified picture of chain motion from the macroscopic to the microscopic scale.

Acknowledgment. We thank the ISIS (Rurtherford Appleton Laboratory, UK) and the Institut Laue Langevin (France) for beam time. S.G. and V.A. acknowledge financial support from EPSRC during the course of the project.

References and Notes

(1) McCrum, N. G.; Read, B. E.; Williams, G. *Anelastic and Dielectric Effects in Polymeric Solids*; Wiley-Interscience: New York, 1967.
(2) Doi, M.; Edwards, S. F. *The Theory of Polymer Dynamics*; Oxford University Press: Oxford, 1986.
(3) Rouse, P. E. *J. Chem. Phys.* **1953**, *21*, 1272.
(4) Kirst, K. U.; Kremer, F.; Pakula, T.; Hollingshurst, J. *Colloid Polym. Sci.* **1994**, *272*, 1420.
(5) Tsagaropoulos, G.; Eisenberg, A. *Macromolecules* **1995**, *28*, 6067.
(6) Litvinov, V. M.; Lavrukhin, B. D.; Zhdanov, A. A. *Polym. Sci. USSR* **1985**, *27*, 2786.
(7) Cosgrove, T.; Griffiths, P. C.; Hollingshurst, J.; Richards, R. D. C.; Semlyen, J. A. *Macromolecules* **1992**, *25*, 6761.
(8) Cosgrove, T.; Turner, M. J.; Griffiths, P. C.; Hollingshurst, J.; Shenton, M. J.; Semlyen, J. A. *Polymer* **1996**, *37*, 1535.
(9) Edwards, C. J. C.; Stepto, R. F. T.; Semlyen, J. A. *Polymer* **1982**, *23*, 869.
(10) Higgins, J. S. In *Static and Dynamic Properties of the Polymeric Solid State*; Pethrick, R. A., Richards, R. W., Eds.; Proceedings of the NATO Advanced Study Institute: Glasgow, 1981.
(11) Higgins, J. S.; Benoit, H. C. *Polymers and Neutron Scattering*; Oxford University Press: Oxford, 1993.
(12) Ewen, B.; Richter, D. *Adv. Polym. Sci.* **1997**, *134*, 1.
(13) Bée, M. *Quasielastic Neutron Scattering: Principles and Applications in Solid State Chemistry, Biology and Materials Science*; Adam Hilger: Bristol, 1988.
(14) Grapengeter, H. H.; Alefeld, B.; Kosfeld, R. *Colloid Polym. Sci.* **1987**, *265*, 226.
(15) Frick, B. In *Non-equilibrium Phenomena in Supercooled Fluids, Glasses and Amorphous Materials*; Giordando, M., Leporini, D., Tosi, M. P., Eds.; World Scientific: Singapore, 1996.
(16) Higgins, J. S.; Ghosh, R. E.; Howells, W. S.; Allen, G. *J. Chem. Soc., Faraday Trans. 2* **1977**, *73*, 40.
(17) Allen, G.; Higgins, J. S.; Maconnachie, A.; Ghosh, R. E. *J. Chem. Soc., Faraday Trans. 2* **1982**, *78*, 2117.
(18) Stuhn, B.; Ewen, B.; Richter, D. *Phys. Rev. B: Condens. Matter* **1985**, *58*, 305.
(19) deGennes, P. G. *Physics* **1967**, *3*, 37. deGennes, P. G. *J. Chem. Phys.* **1971**, *55*, 572.
(20) Richter, D.; Ewen, B. *Prog. Colloid Polym. Sci.* **1989**, *80*, 53.
(21) Arbe, A.; Monkenbusch, M.; Stellbrink, J.; Richter, D.; Farago, B.; Almdal, K.; Faust, R. *Macromolecules* **2001**, *34*, 1281.
(22) Arrighi, V.; Gagliardi, S.; Higgins, J. S. *Mater. Res. Soc. Symp.* **2001**, *661*, KK4.4.1.
(23) Ganazzoli, F.; Raffaini, G.; Arrighi, V. *Phys. Chem. Chem. Phys.* **2002**, *4*, 3734.
(24) Ngai, K. L.; Colmenero, J.; Alegria, A.; Arbe, A. *Macromolecules* **1992**, *25*, 6727.
(25) Ganazzoli, F.; Allegra, G.; Higgins, J. S.; Roots, J.; Brückner, S.; Lucchelli, E. *Macromolecules* **1985**, *18*, 435.
(26) Harnau, L.; Winkler, R. G.; Reineker, P. *J. Chem. Phys.* **1997**, *106*, 2469.
(27) Allegra, G.; Ganazzoli, F. *J. Chem. Phys.* **1981**, *74*, 1310.
(28) Allegra, G.; Ganazzoli, F. *Adv. Chem. Phys.* **1989**, *75*, 265.
(29) Allegra, G.; Higgins, J. S.; Ganazzoli, F.; Lucchelli, E.; Brückner, S. *Macromolecules* **1984**, *17*, 1253.
(30) Arrighi, V.; Ganazzoli, F.; Zhang, C.; Gagliardi, S. *Phys. Rev. Lett.* **2003**, *90*, 058301.
(31) Chahid, A.; Alegría, A.; Colmenero, J. *Macromolecules* **1994**, *27*, 4421.
(32) Frick, B.; Fetters, L. J. *Macromolecules* **1994**, *27*, 974.
(33) Arrighi, V.; Higgins, J. S.; Burgess, A. N.; Howells, W. S. *Macromolecules* **1995**, *28*, 2745.
(34) Williams, G.; Watts, D. C. *Trans. Faraday Soc.* **1970**, *66*, 80.
(35) Lindsey, C. P.; Patterson, G. D. *J. Chem. Phys.* **1980**, *73*, 3348.
(36) Shmidt, C.; Kuhn, K. J.; Spiess, H. W. *Prog. Colloid Polym. Sci.* **1985**, *71*, 71.
(37) Mukhopadhyay, R.; Alegria, A.; Colmenero, J.; Frick, B. *Macromolecules* **1998**, *31*, 3985.
(38) Zorn, R.; Frick, B.; Fetters, L. J. *J. Chem. Phys.* **2002**, *16*, 845.
(39) Wehrle, M.; Hellmann, G. P.; Spiess, H. W. *Colloid Polym. Sci.* **1987**, *265*, 815.
(40) Arrighi, V.; Higgins, J. S. *Physica B* **1996**, *226*, 1.
(41) Colmenero, J.; Alegria, A.; Alberdi, J. M.; Alvarez, F.; Frick, B. *Phys. Rev. B* **1991**, *44*, 7321.
(42) Colmenero, J.; Alegria, A.; Arbe, A.; Frick, B. *Phys. Rev. Lett.* **1992**, *69*, 478.
(43) Alvarez, F.; Arbe, A.; Colmenero, J. *Chem. Phys.* **2000**, *261*, 47.
(44) Allegra, G.; Ganazzoli, F. *Macromolecules* **1981**, *14*, 1110.
(45) Allegra, G. *J. Chem. Phys.* **1974**, *61*, 4910; *J. Chem. Phys.* **1975**, *63*, 599.
(46) Flory, P. J. *Statistical Mechanics of Chain Molecules*; Wiley & Sons: New York, 1969.
(47) Mattice, W. L.; Suter, U. W. *Conformational Theory of Large Molecules*; Wiley-Interscience: New York, 1994.
(48) Bahar, I.; Zuniga, I.; Dodge, R.; Mattice, W. L. *Macromolecules* **1991**, *24*, 2986, 2993.
(49) Flory, P. J.; Crescenzi, V.; Mark, J. E. *J. Am. Chem. Soc.* **1964**, *86*, 146.
(50) Telling, M. T. F.; Howells, W. S. *GUIDE−IRIS Data Analysis*, RAL-TR-2000-004, Rutherford Appleton Laboratory, 2000.
(51) Howells, W. S. *A Fast Fourier Transform Program for the Deconvolution of IN10 Data*, RL-81-039, Rutherford Appleton Laboratory, 1981.
(52) Randl, O. G. *SQW User Manual*, Institut Laue-Langevin, 1995.
(53) Arrighi, V.; Higgins, J. S. *J. Chem. Soc., Faraday Trans.* **1997**, *93*, 1605.
(54) Fox, T. G.; Allen, V. R. *J. Chem. Phys.* **1965**, *41*, 344.
(55) Dvornic, P. R.; Jovanovic, J. D.; Govedarica, M. N. *J. Appl. Polym. Sci.* **1993**, *49*, 1497.
(56) Ghannam, M. T.; Esmail, M. N. *Ind. Eng. Chem. Res.* **1998**, *37*, 1335.
(57) Ferry, J. B. *Viscoelastic Properties of Polymers;* John Wiley & Sons: New York, 1970.
(58) Barlow, A. J.; Harrison, G.; Lamb, J. *Proc. R. Soc. London* **1964**, *282*, 228.
(59) Henry, A. W.; Safford, G. J. *J. Polym. Sci.* **1976**, *14*, 1077.
(60) Allen, G.; Wright, C. J.; Higgins, J. S. *Polymer* **1974**, *15*, 319.
(61) Amaral, L. W.; Vinhas, L. A.; Herdade, S. B. *J. Polym. Sci., Polym. Phys.* **1976**, *14*, 1077.
(62) Allen, G.; Brier, P. N.; Goodyear, G.; Higgins, J. S. *Faraday Symp. Chem. Soc.* **1972**, *6*, 169.
(63) Allen, G.; Ghosh, R. E.; Heidemann, A.; Higgins, J. S.; Howells, W. S. *Chem. Phys. Lett.* **1974**, *27*, 308.
(64) Allen, G.; Higgins, J. S.; Wright, C. J. *J. Chem. Soc., Faraday Trans. 2* **1974**, *70*, 348.

MA034843X